Positronium Rydberg excitation diagnostic in a 1T cryogenic environment

Cite as: AIP Conference Proceedings **2182**, 030002 (2019); https://doi.org/10.1063/1.5135825
Published Online: 27 December 2019

R. Caravita, S. Mariazzi, S. Aghion, C. Amsler, M. Antonello, A. Belov, G. Bonomi, R. S. Brusa, M. Caccia, A. Camper, F. Castelli, G. Cerchiari, D. Comparat, G. Consolati, A. Demetrio, L. Di Noto, M. Doser, C. Evans, M. Fanì, R. Ferragut, J. Fesel, A. Fontana, S. Gerber, M. Giammarchi, A. Gligorova, F. Guatieri, P. Hackstock, S. Haider, A. Hinterberger, H. Holmestad, A. Kellerbauer, O. Khalidova, D. Krasnický, V. Lagomarsino, P. Lansonneur, P. Lebrun, C. Malbrunot, J. Marton, V. Matveev, S. R. Müller, G. Nebbia, P. Nedelec, M. Oberthaler, D. Pagano, L. Penasa, V. Petracek, F. Prelz, M. Prevedelli, B. Rienaecker, J. Robert, O. M. Røhne, A. Rotondi, H. Sandaker, R. Santoro, L. Smestad, F. Sorrentino, G. Testera, I. C. Tietje, M. Vujanovic, E. Widmann, P. Yzombard, C. Zimmer, J. Zmeskal, and N. Zurlo

Positronium Rydberg excitation diagnostic in a 1T cryogenic environment

R. Caravita[1,a)], S. Mariazzi[2,3,b)], S. Aghion[4,5], C. Amsler[6], M. Antonello[5,7], A. Belov[8], G. Bonomi[9,10], R. S. Brusa[2,3], M. Caccia[5,7], A. Camper[1], F. Castelli[5,11], G. Cerchiari[12], D. Comparat[13], G. Consolati[4,5], A. Demetrio[14], L. Di Noto[15,16], M. Doser[1], C. Evans[4,5], M. Fanì[1,15,16], R. Ferragut[4,5], J. Fesel[1], A. Fontana[10], S. Gerber[1], M. Giammarchi[5], A. Gligorova[6], F. Guatieri[2,3], P. Hackstock[6], S. Haider[1], A. Hinterberger[1], H. Holmestad[1], A. Kellerbauer[12], O. Khalidova[1], D. Krasnický[16], V. Lagomarsino[15,16], P. Lansonneur[17], P. Lebrun[17], C. Malbrunot[1,6], J. Marton[6], V. Matveev[8,18], S. R. Müller[14], G. Nebbia[19], P. Nedelec[17], M. Oberthaler[14], D. Pagano[9,10], L. Penasa[2,3], V. Petracek[20], F. Prelz[5], M. Prevedelli[21], B. Rienaecker[1], J. Robert[13], O. M. Røhne.[22], A. Rotondi[10,23], H. Sandaker[22], R. Santoro[5,7], L. Smestad[1,24], F. Sorrentino[15,16], G. Testera[16], I. C. Tietje[1], M. Vujanovic[1], E. Widmann[6], P. Yzombard[12], C. Zimmer[1,12,25], J. Zmeskal[6] and N. Zurlo[10,26]

[1]*Physics Department, CERN, 1211 Geneva 23, Switzerland*
[2]*Department of Physics, University of Trento, via Sommarive 14, 38123 Povo, Trento, Italy*
[3]*TIFPA/INFN Trento, via Sommarive 14, 38123 Povo, Trento, Italy*
[4]*Politecnico of Milano, Piazza Leonardo da Vinci 32, 20133 Milano, Italy*
[5]*INFN Milano, via Celoria 16, 20133, Milano, Italy*
[6]*Stefan Meyer Institute for Subatomic Physics, Austrian Academy of Sciences, Boltzmanngasse 3, 1090 Vienna, Austria*
[7]*Department of Science, University of Insubria, Via Valleggio 11, 22100 Como, Italy*
[8]*Institute for Nuclear Research of the Russian Academy of Science, Moscow 117312, Russia*
[9]*Department of Mechanical and Industrial Engineering, University of Brescia, via Branze 38, 25123 Brescia, Italy*
[10]*INFN Pavia, via Bassi 6, 27100 Pavia, Italy*
[11]*Department of Physics, University of Milano, via Celoria 16, 20133 Milano, Italy*
[12]*Max Planck Institute for Nuclear Physics, Saupfercheckweg 1, 69117 Heidelberg, Germany*
[13]*Laboratoire Aimé Cotton, Université Paris-Sud, ENS Cachan, CNRS, Université Paris-Saclay, 91405 Orsay Cedex, France*
[14]*Kirchhoff-Institute for Physics, Heidelberg University, Im Neuenheimer Feld 227, 69120 Heidelberg, Germany*
[15]*Department of Physics, University of Genova, via Dodecaneso 33, 16146 Genova, Italy*
[16]*INFN Genova, via Dodecaneso 33, 16146 Genova, Italy*
[17]*Institute of Nuclear Physics, CNRS/IN2p3, University of Lyon 1, 69622 Villeurbanne, France*
[18]*Joint Institute for Nuclear Research, 141980 Dubna, Russia*
[19]*INFN Padova, via Marzolo 8, 35131 Padova, Italy*
[20]*Czech Technical University, Prague, Bøehová 7, 11519 Prague 1, Czech Republic*
[21]*University of Bologna, Viale Berti Pichat 6/2, 40126 Bologna, Italy*
[22]*Department of Physics, University of Oslo, Semælands vei 24, 0371 Oslo, Norway*
[23]*Department of Physics, University of Pavia, via Bassi 6, 27100 Pavia, Italy*

The 18th International Conference on Positron Annihilation (ICPA-18)
AIP Conf. Proc. 2182, 030002-1–030002-6; https://doi.org/10.1063/1.5135825
Published by AIP Publishing. 978-0-7354-1929-2/$30.00

[24]*The Research Council of Norway, P.O. Box 564, NO-1327 Lysaker, Norway*
[25]*Department of Physics, Heidelberg University, Im Neuenheimer Feld 226, 69120 Heidelberg, Germany*
[26]*Department of Civil Engineering, University of Brescia, via Branze 43, 25123 Brescia, Italy*

[a)]corresponding author, ruggero.caravita@cern.ch
[b)]corresponding author, mariazzi@science.unitn.it

Abstract. Forming a pulsed beam of cold antihydrogen using charge-exchange with Rydberg positronium (Ps) is the goal of the AEḡIS collaboration, which aims to a first gravity measurement on neutral antimatter. Recently achieved results in Ps formation and laser spectroscopy in the main AEḡIS apparatus are summarized. First, Ps has been produced using nanochanneled silicon targets in a cryogenic environment ($\sim$ 15 K) with 1 T magnetic field and observed by means of Single-Shot Positron Annihilation Lifetime Spectroscopy. The first demonstration of Ps n=3 excitation has been obtained as well using the same technique, validating the proof-of-concept of AEgIS. Subsequently, a new fast and high sensitivity detection method for laser-excited Ps in high magnetic field has been developed, using the combination of laser/field ionization and an high sensitivity MCP detector coupled to a low-noise CMOS camera. This technique will form the basis of future experiments involving Rydberg Ps spectroscopy in AEḡIS.

INTRODUCTION

Measuring directly gravity on a pulsed beam of cold antihydrogen ($\bar{H}$) is the ambitious goal of the AEgIS collaboration [1], aiming to observe the free-fall parabolic trajectory of a cloud of $\bar{H}$ atoms in a constant (Earth's) gravitational field using a moiré deflectometer [2]. The scheme chosen by AEgIS to produce a pulsed source of $\bar{H}$ is based on a double charge-exchange reaction between cold trapped antiprotons ($\bar{p}$) and laser excited Rydberg Positronium (Ps) atoms, first demonstrated experimentally by the ATRAP collaboration [3]:

$$\bar{p}^- + Ps^* \longrightarrow \bar{H}^* + e^- . \tag{1}$$

One of the most crucial aspects towards producing such a source consists in developing a fast and sensitive diagnostic of Ps laser excitation in the cryogenic and high magnetic field environment of AEḡIS, able to characterize the angular and velocity distribution of Ps atoms produced by its cryogenic target as they fly through the antihydrogen production trap and monitor reliably the excitation by the laser.

EXPERIMENTAL

A scheme of the current setup of the experiment is shown in Figure 1. A Ps converter made of nanochanneled mesoporous silicon [4] is placed $\sim$ 1.7 cm above the plasma of trapped $\bar{p}$ prepared using two sets of Malmberg-Penning traps: the $\bar{p}$ catching traps, placed in a 4.5 T magnetic field region, and the $\bar{H}$ production trap, placed in a 1 T magnetic field. The electrodes of the production trap are custom designed with an entrance grid on the upper side to let Ps^* atoms fly inside the trap. Ps is produced implanting positrons (e^+) with keV energy inside the converter, where ground state Ps atoms (142 ns lifetime) are produced with high efficiency [5] and diffuse in the nanochannels loosing energy by collisions [6]. They finally are re-emitted into vacuum with an overall efficiency at room temperature up to 50% [7].

Two pulses of laser radiation from AEḡIS laser system (described in the details in [8]) are sent from the side of the converter synchronously and with tunable delay with respect to the e^+ implantation instant to excite the emitted fraction of ortho-Ps to Rydberg levels using a two step excitation scheme. An UV 205.045 nm laser pulse drives the $1 \rightarrow 3$ transition, whereas an IR 1700 nm pulse conveys the atoms to $n = 15 - 23$ [9, 8] and an intense IR pulse at 1064 nm is optionally used for selective photoionization of $n = 3$. The total lifetime of Ps^* atoms is much higher than Ps (tens of μs to ms), allowing the atoms to reach the $\bar{p}$ production trap without annihilating in-flight.

Positrons are produced, moderated and accumulated up to many minutes in the AEḡIS positron system (see [7] for the details). e^+ clouds are extracted from the accumulator with $\sim$ 300 eV energy and $\sim$ 20 ns time length and are guided towards the main 4.5 T magnetic field of AEḡIS antiproton catching traps through a 45°-tilted $0.05 - 0.25$ T transfer line [10] comprising a 60 cm pulsed HV electrode, which increases their energy to 4.6 keV and time-compresses them to < 10 ns [11] (see Figure 1). The bunches, guided by the 4.5 T and 1.0 T magnetic fields, are steered on the target by means of two couples of vertical and horizontal correction coils in anti-Helmholtz configuration at the end of the transfer line. The precise alignment is done with the imaging feedback given by an Hamamatsu F2222 two-stage

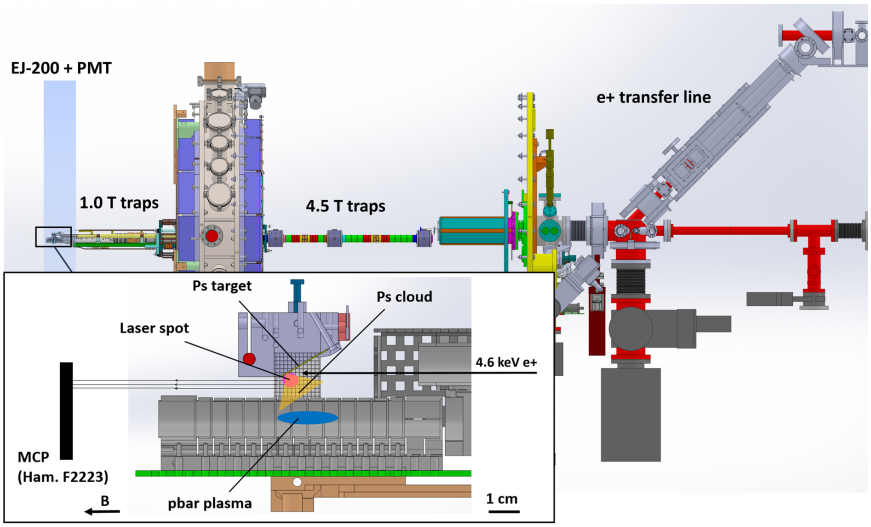

Figure 1. Schematic drawing of AEGIS experimental layout to produce antihydrogen by charge exchange with Rydberg-excited positronium. The main elements described in the text are marked. Inset: zoom of the $\bar{H}$ production region.

micro-channel plate (MCP) assembly with a P46 phosphor screen imaged by an Hamamatsu ORCA-Flash4 CMOS camera (Figure 1, inset), detecting the tails of the cloud annihilating on its front surface after traversing the whole AEgIS trap stack.

A semi-cylindrical slab of EJ200 plastic scintillator wrapped around the experiment cryostat (70 cm internal radius, 10 cm height, 1 cm thickness and 120°coverage in the azimuthal angle for a total solid angle coverage of $\sim 2.38\%$), coupled with a 20 cm pyramidal light guide to a μmetal shielded EMI 9954B photomultiplier tube (PMT) was used to detect the time distribution of photons emitted by the e^+ and Ps annihilations. The electrical signal of the PMT was split by a Mini-Circuits ZFRSC-2050B 50%-50% splitter and digitized with two channels of a 12bit, 1.0 GHz HDO4096 LeCroy oscilloscope set at high (50 mV/div) and low (1 V/div) resolutions (similarly to the setup used in [12]).

Ps DETECTION WITH SCINTILLATION DETECTORS

The formation of Ps from the cryogenic target inside AEgIS and its laser excitation to the $n = 3$ level were first observed by means of Single-Shot Positron Annihilation Lifetime Spectroscopy (SSPALS) [9, 12]. The experiments were conducted as follows.

Two families of ~ 100 shots each were acquired respectively with the e^+ aligned on the target and on the MCP metallized front face (a Ni-Al alloy), where formation of Ps was inhibited. Two SSPALS spectra with and without Ps formation (Figure 2, left panel) were built averaging the signals recorded from the scintillator in each family. These spectra show a peak at 0 ns, due to prompt annihilations of e^+ in the target, and a long tail structure at later times partly due to retarded fluorescence of the plastic scintillator and partly due to Ps annihilations.

The relative difference S between the integrals of the SSPALS spectra in the window $150 - 500$ ns evidences an increase $S^{prod} = 1 - A^{prod}_{target}/A^{prod}_{MCP} = 37 \pm 2\%$. The amount of produced Ps can be estimated by two methods. The first is to consider the relative decrease of the prompt peak amplitude when Ps is formed with respect to annihilations on the MCP surface. This methods gives a lower estimate of the Ps production efficiency, due to possible PMT non-linearities close to saturation. The second method consists in evaluating the ratio between the integral of the two curves' difference in the window $150 - 500$ ns (which is mostly due to 3γ annihilation events in vacuum) and the integral of the whole curve in absence of Ps formation (mostly due to 2γ annihilation events on surfaces), multiplied by $2/3$ to account for the different number of gamma rays produced in each annihilation event. This method relies on the assumption of flat efficiency and energy response of the scintillation detector to γ-rays emitted form para-Ps and ortho-Ps annihilations. This is a good first approximation, as the EJ-200 scintillation material (having low-Z and low density) operates exclusively by the Compton effect with negligible photo-peak. In fact, this method is expected

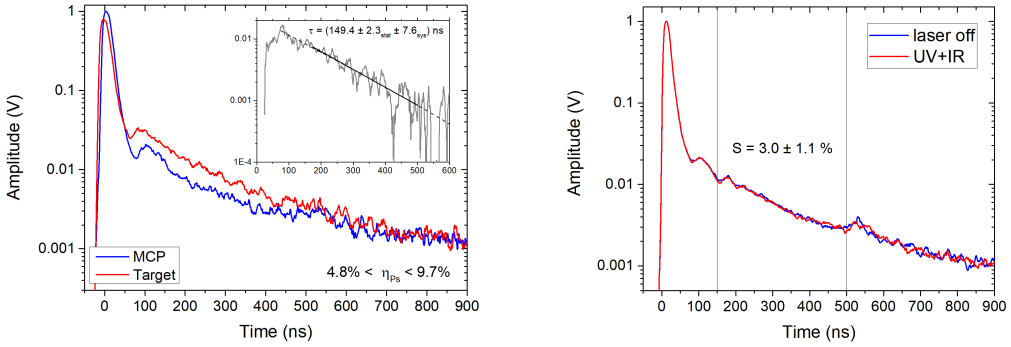

Figure 2. Left panel: average SSPALS spectra of e^+ annihilating on the MCP (blue) and on the target showing Ps formation (red) and the negative exponential fit of the difference used to estimate the lifetime and the Ps yield (in inset). Right panel: SSPALS spectrum obtained introducing the $n = 3$ excitation and photoionization laser (red) compared to the case without the lasers (blue); the interval used for the relative difference estimation is highlighted.

to be slightly over-estimating to the amount of formed Ps, as the scintillation material response is 10-20 % higher for 300 keV γ-rays versus 511 keV γ-rays. These two estimates indicate that the yield of the e^+/Ps converter in the AEgIS experimental configuration lies in the range $\eta_{prod} = (4.8 - 9.7)$ % due to the present limitation in temperature treating the target to an higher temperature than $\sim 0\,^{\circ}$C [13]. The lifetime obtained from an exponential fit of their difference (Figure 2, left inset) was found compatible with the expected Ps lifetime: $149.4 \pm 2.3_{\text{stat}} \pm 7.6_{\text{sys}}$ ns.

The introduction of the pulsed 205.045 nm laser for the $1 - 3$ excitation (thoroughly described in [9] and [8]), superimposed with an intense 1064 nm laser pulse for selectively photoionizing $n = 3$ caused a reduction of the Ps signal in the Ps tail of $S^{photo} = 1 - A_{on}^{photo}/A_{off}^{photo} = 3.0 \pm 1.1\%$ in the same analysis window (Figure 2, right panel). ~ 400 shots per family were used for this experiment. This found value can be converted in terms of relative amount of Ps by normalizing it to S^{form}, which represent the total amount of signal in the tail that can be ascribed to Ps. Thus the laser excitation efficiency is found to be roughly $\eta_{laser} = S^{photo}/S^{form} = 8.1 \pm 3.0\%$, close to the result obtained in a similar experiment conducted in a dedicated setup with the same type of targets [9].

A FAST IMAGING DETECTOR FOR Ps SPECTROSCOPY IN MAGNETIC FIELDS

The main limitation of SSPALS applied to Ps laser excitation diagnostics in AEgIS complex experimental geometry is the long measurement time required to reach a sufficiently high signal-to-noise ratio to distinguish the effect of laser on the Ps sample ($S/N \sim 3$ in the case of Figure 2 right panel, corresponding to ~ 16 h of measurements), which imposes severe limitations to the experiments that can be performed. This motivated the developing of an alternative, faster diagnostics for Ps laser excitation, based on the highly sensitive MCP detector amplifying the charged e^+ produced from photo-/field-ionization of Ps and guided by the 1.0 T magnetic field.

Indeed, Ps could be dissociated either from $n = 3$ by laser photoionization (using both 205.045 nm and 1064 nm pulsed lasers) or in high Rydberg states $n > 17$ by self-ionization in the high magnetic field, i.e. caused by the self-induced motional Stark electric field $\vec{E}_{MS} = \vec{v}_{Ps} \times \vec{B} \approx 10^5 \cos(\theta_{Ps})\vec{x}$ V m^{-1} felt by the Rydberg atoms in their co-moving frame of reference [14]. The dissociated e^+ and e^- are bound to their magnetic field line guiding them to the front face of the MCP (Figure 1, inset) with an energy roughly given by the binding energy of the initial state $6.8\,\text{eV}/n^2$ (the initial kinetic energy of the Ps atom is negligible, ≈ 60 meV for 10^5 m s^{-1} Ps). An intrinsic imaging resolution limit is set by the size of the e^+ orbit, which is given by the gyro-radius $r = m_e v_\perp / e_0 B \approx 0.5$ µm for $v_\perp = 10^5$ m s^{-1} in the 1.0 T field of AEgIS, much smaller than the interdistance between MCP micro-channels (usually around 10 µm).

The Ps target holder was thus modified with respect to the original AEgIS configuration [15] to minimize the distance between the lower end of the silica target and the view volume of the MCP and to allow the lasers to be aligned at a lower position with respect to the e^+ implantation axis, in view of the MCP front surface (see Figure 1, inset). Resulting e^+ were separated from e^- applying a constant 10 V cm^{-1} axial electric field using the nearby production trap electrodes. Moreover, to reach the nominal detection efficiency of the MCP for e^+, its metallized front face was

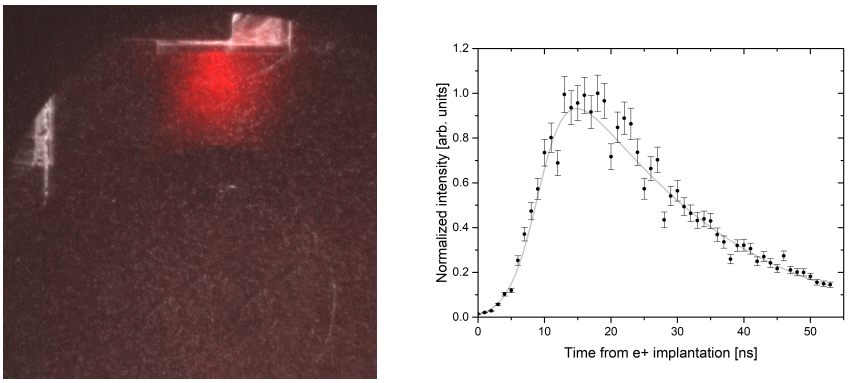

Figure 3. Left panel: pictorial color superposition of the electron background on the MCP obtained shining the UV laser without any blocking electric field (in gray) with the average of 50 measurements of photoionized $n = 3$ Ps (in red), showing the Ps imaging capability of this detection method. The upper square structure is the silicon target; the left white structure is the grid covering the laser alignment screen; the bottom ring structure is the inner radius of the production trap electrodes. Right panel: an example measurement obtained with this technique: normalized integrated intensity on the image as a function of the e^+ implantation time (the double logistic fit is a guide for the eye).

biased to −180 V.

Results obtained with this technique show a signal-to-noise ratio of about ∼ 150 (roughly a 50-fold gain with respect to SSPALS applied to Ps $n = 3$ photoionization) averaging just 5 images obtained with the UV and photoionization lasers and the MCP front face kept at −180 V, MCP back face at −1.2 kV and the phosphor screen at −4.2 kV (also thanks to the low shot noise of the ORCA-Flash4 water-cooled CMOS). Also, the required ∼ 10 min of e^+ accumulation correspond to a 100-fold gain in terms of reduced measurement time. An example Ps distribution obtained averaging 50 images with uniformly distributed laser wavelengths, to cancel the Doppler selection due to the limited 120 GHz bandwidth of the UV laser, is shown in Figure 3, left panel. Figure 3, right panel, shows an example of the high-quality measurements that can be obtained with this technique. In the specific, the integrated image intensity is shown as a function of the e^+ implantation time, obtained in steps of 1 ns and averaging 10 images per point (roughly 9 h of measurement time). The measured intensity of each image was multiplied by $e^{t/142\,\mathrm{ns}}$ to account for the finite Ps lifetime, where t is the delay from the positron implantation instant.

CONCLUSIONS

The formation of positronium from AEḡIS 1.0 T cryogenic target was first detected by means of the SSPALS technique using a plastic scintillation detector. SSPALS allowed to estimate the e^+-Ps conversion efficiency to be ∼ 9%. Laser excitation to $n = 3$ was also demonstrated with the same technique, despite its low signal-to-noise ratio due to the geometrical limitations of the AEḡIS setup. Subsequently, a new detection method for ionized Ps in high magnetic field based on a MCP detector was developed. This method demonstrated to be roughly 100 times faster and 50 times more sensitive than SSPALS to laser-Ps signals, opening the way to future high-sensitivity Ps measurements in AEḡIS (such as the full characterization of Ps angular and velocity distributions from the cryogenic target or Rydberg spectroscopy in a 1 T field) and providing a valuable and online shot-by-shot diagnostics of Ps Rydberg excitation for pulsed antihydrogen production.

References

[1] Kellerbauer, A. et al. (AEgIS collaboration), NIM B **266**, 351–356 (2008).
[2] S. Aghion et al. (AEgIS collaboration), Nat. Commun. **5**, p. 4538 (2014).
[3] C. H. Storry et al. (ATRAP collaboration), Phys. Rev. Lett. **93** (2004).
[4] S. Mariazzi, P. Bettotti, and R. S. Brusa, Phys. Rev. Lett. **104**, p. 243401 (2010).
[5] S. Mariazzi, P. Bettotti, S. Larcheri, L. Toniutti, and R. S. Brusa, Phys. Rev. B **81**, p. 235418 (2010).
[6] S. Mariazzi, A. Salemi, and R. S. Brusa, Phys. Rev. B **78** (2008).

[7] S. Aghion et al. (AEgIS collaboration), NIM B **362**, 86–92 (2015).
[8] S. Cialdi, I. Boscolo, F. Castelli, F. Villa, G. Ferrari, and M. Giammarchi, NIM B **269**, 1527 – 1533 (2011).
[9] S. Aghion et al. (AEgIS collaboration), Phys. Rev. A **94**, p. 012507 (2016).
[10] D. Krasnický, Master's thesis, Czech Technical University in Prague (2009).
[11] R. Caravita, Ph.D. thesis, Università degli Studi di Genova 2017.
[12] S. Aghion et al. (AEgIS collaboration), Phys. Rev. A **98**, p. 013402 (2018).
[13] B. S. Cooper et al., Phys. Rev. B **93**, p. 125309 (2016).
[14] D. B. Cassidy, Eur. Phys. J. D **72**, p. 53 (2018).
[15] R. Caravita et al. (AEgIS collaboration), Acta Phys. Polon. B **48**, p. 1583 (2017).